



Study of Surface Roughness on Friction in Rolling/Sliding Contacts: Ball-on-Disc Versus Twin-Disc

Ellen Bergseth¹ · Yi Zhu² · Anders Söderberg¹

Received: 30 September 2019 / Accepted: 19 May 2020 / Published online: 28 May 2020
© The Author(s) 2020

Abstract

Although the efficiency of a gear pair is currently high, a better understanding of surface/lubricant contribution on efficiency is critical. Electrified drivelines will, for example, impose higher speed and alternate loading, and it is expected that these new conditions will, to a greater extent, rely on the surface/lubricant characteristics. Phenomena taking place in the gear contact is often measured using ball-on-disc and twin-disc tribometers. In this study, these two test set-ups were compared in order to assess differences in the behaviour of surface/lubricant interactions. Results showed that ball-on-disc and twin-disc set-ups reflect the same friction trends. However, the friction results differed by a factor of roughly two, even though the tribometers were set-up to run at the same contact pressure. The wear mechanisms also differed: micropits occurred on discs used in the twin-disc set-up, whereas normal or no wear was found on the ball-on-disc specimens. The contact conditions for the two test set-ups were also analysed using a numerical model. The comparison of these two machines may aid gear designers in selecting the proper experimental set-up for their purpose.

Keywords Ball-on-disc · Twin-disc · Surface roughness · Contact analysis

List of symbols

A	Hertzian contact area (mm ²)
A_r	Real contact area (mm ²)
C^p	Matrix of the influence coefficients for normal contact
C^q	Matrix of the influence coefficients for tangential contact
c_0	Integration constant for calculating tangential contact
F_N	Normal force (N)
F_T	Tangential force (N)
h	Vector containing the gaps between the cells before loading (mm)
n	Number of cells
p	Vector containing the unknown pressures (MPa)
p_0	Maximum nominal contact pressure (MPa)
q	Traction (MPa)
Ra	Average roughness parameter (μm)

Rq	RMS roughness (μm)
r	Radius of curvature (mm)
s	Slip distance (mm)
u	Deformation (mm)
v	Speed (mm/s)
x	Distance to leading edge (mm)
δ_z	Applied normal displacement (mm)
ξ	Slip (%)
μ	Friction or traction coefficient
σ	Standard deviation

Index

a, b	Body a, b
c	Computational
i, j	Indices
l	Limiting coefficient of friction
x	Direction of motion
y	Direction perpendicular to motion
z	Normal direction

✉ Ellen Bergseth
bergseth@kth.se

¹ KTH Royal Institute of Technology, Machine Design, Brinellvägen 83, Stockholm, Sweden

² Zhejiang University, Zheda Road 38, Hangzhou 310027, China

1 Introduction

The rolling/sliding gear contact is often simulated using ball-on-disc and twin-disc machine, in which both components are driven by separate motors. These machines

facilitate control of factors that influence the results, including contact load, radii, entrainment speed, and slide-to-roll ratio (or slip), all of which constantly change along the gear line of action. The shortcoming of both configurations is that the cyclic nature of the gear contact is replaced by steady conditions. The advantage of a twin-disc set-up is that the scaling of the contact (i.e. the reduced radius of curvature proportions) can be set closer to those in a real gear contact. Moreover, the twin-disc set-up is generally said to properly simulate the friction behaviour trends in real gears [1, 2]. On the other hand, the specimens used in a ball-on-disc set-up can be less expensive, and the size of the machine allows bench testing. In addition, there are no alignment issues, which can be hard to control in a twin-disc machine. Ball-on-disc has proven to be a reasonable way to understand the performance of gear oils, Björling et al. [3] show that ball-on-disc measurements can capture same friction performance of lubricants as FZG gear test device.

There are several ball-on-disc machine manufacturers. Vengudusamy et al. [4] studied the impact of contact conditions on friction properties of gear oils in two ball-on-disc machines, Mini Traction Machine (MTM) and Schwing-Reib-Verschleiss (SRV) tribometer. They discuss differences in friction due to test configurations; contact pressure appears to show similar effects on friction in the mixed lubrication regime in both set-ups. Another ball-on-disc machine, for evaluating contact friction behaviour to oil parameters, is the Wedeven Associates Machine (WAM) [3, 5].

In many studies in which the gear and also wheel-rail contact is simulated using these test set-ups, the main topographical orientation is in the direction of sliding (circumferential grinding), rather than perpendicular to sliding (transverse grinding) as in real ground gears. Tool configuration makes it slightly more complicated to manufacture test specimens with the grinding marks running in the transverse direction, but not doing so affects the lubricant film formation and moves testing conditions farther away from those of real ground gears. Höhn et al. [6] found experimentally in a twin-disc set-up (run in the elastohydrodynamic regime) that surfaces generated by transverse grinding showed almost no relationship between roughness and film thickness, unlike circumferential grinding.

The purpose of this paper is to compare two test set-ups, ball-on-disc and twin-disc, and highlight the differences in the behaviour of surface/lubricant interactions using these two test machines. Two surface finishes (i.e. ground or polished surface roughness), each run with two formulated lubricants, an ester-based environmentally adapted lubricant (EAL) and a commercial PAO-based lubricant. The work partly builds on one of the authors' previous studies with the same set of lubricants and surfaces (Bergseth et al. [7]). The reader is referred to that publication for more results on the frictional and wear performance of surfaces in twin-disc

tests only. However, this paper presents the key results from the previous study. With this in mind, the test conditions are as close as possible. The fact that the results obtained with the ball-on-disc did not wholly match the results of the previous twin-disc machine led to this investigation. The contact conditions for the two test set-ups were also compared using a numerical model.

2 Methods

2.1 Test Equipment

A ball-on-disc machine (Mini Traction Machine) was used to simulate a rolling/sliding gear contact. A schematic view of the test machine is shown in Fig. 1. This test configuration can load 5 to 75 N. Contact pressures can range from 0 to 1.25 GPa with standard ball specimens and up to 3.1 GPa with alternative specimens; thus instead of a ball, a crowned roller (i.e. barrel) was used in this study in order to reach the desired contact pressure. The speed range for the machine is from -4 to 4 m/s. The barrel (or ball) is loaded at an angle to the disc, and the barrel and disc are driven by two separate motors. The disc is submerged in a lubricant bath that is temperature controlled by a silicone oil cooler to within ± 1 °C during testing. The vertical shaft and drive systems that support the disc are fixed, but the shaft and drive system that supports the upper specimen is supported by a gimbal arrangement. The lateral force exerted on the barrel is measured using a force transducer that further provides the coefficient of friction. All test parameters such as load, speed, and temperature are controlled by a computer. Stribeck curves were created by increasing the rolling speed keeping temperature, slip, and normal load constant. Friction is measured at each step by using the average value of friction forces from two measurements using positive (disc moving faster than barrel) and negative (barrel moving faster than disc) slip. This procedure removes offset errors in the friction measurements.

2.2 Test Specimens

The ball-and-disc test specimens used are shown in Fig. 2 together with twin-disc specimens for comparison. The barrels, with an outside diameter of 17.48 mm and fillet radius of 1 mm, were made of standard 100Cr6 bearing steel (750 HV \approx 60 HRC) and were used as-manufactured from the supplier. The disc surfaces, with an outside diameter of 46 mm, were made of 16MnCr5 carburised gear steel, with a case depth of 1 mm and surface hardness 60 ± 2 HRC. After hardening the disc surfaces were produced by either transverse grinding, circumferential grinding, or polishing. The three surface types will be referred to as 'transverse

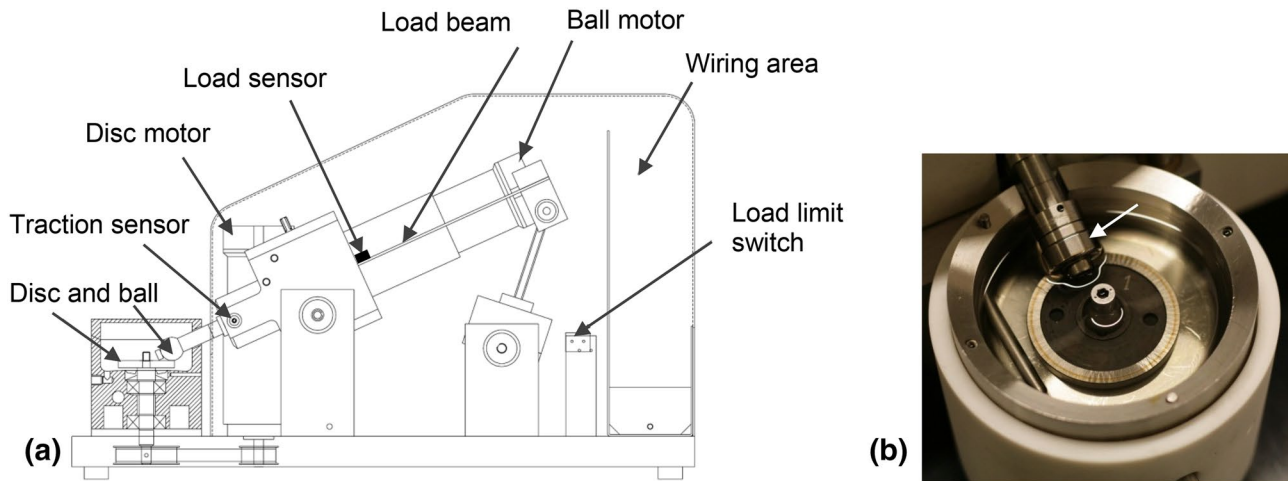


Fig. 1 Schematic view of the test machine where standard specimen ball instead of a barrel is mounted on the shaft (a) and a photo of the test set-up (b). The barrel is indicated with a white arrow

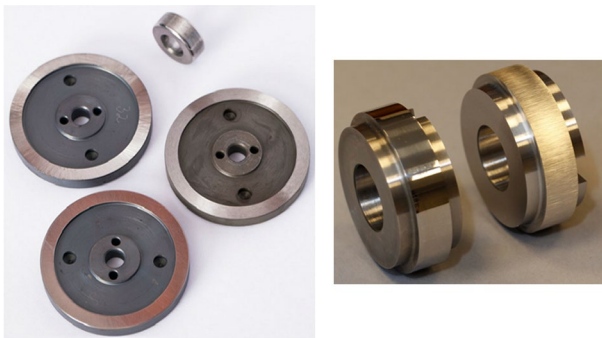


Fig. 2 Three discs with three different surface topographies and one barrel used for ball-on-disc testing and two discs (polished and ground, respectively) for twin-disc testing

ground', 'circumferential ground', and 'polished' throughout this paper. The surface topography was measured with a stylus instrument, a Taylor Hobson Form Talysurf PGI 800. This equipment is traceable to national standards and has a stylus tip radius of 2 μm . The mean average roughness R_a is 0.97 μm for the transverse and circumferential ground and 0.05 μm for the polished. The mean root mean square roughness R_q is 1.1 μm for the transverse and circumferential ground and 0.06 μm for the polished. The mean maximum peak height R_p is 2.3 μm for the transverse and 2.1 μm for the circumferential, R_p is 0.10 μm for the polished. Measurements made use of Gaussian filtering and an upper cut-off of 0.8 mm. To gain a better view of the surface topographies, 3D measurements were made using the same stylus device, as shown in Fig. 3.

The characteristics of the lubricants are shown in Table 1. The commercial lubricant is a commercial heavy truck gearbox lubricant and the EAL-based oil was "tuned" to perform

as the commercial lubricant but at the same time be more sustainable. Both the formulated gear lubricants used are synthetic of GL-4 performance level and 75 W/85 viscosity grade. The EAL base is a saturated mixture of esters, while the commercial lubricant having a polyalphaolefin (PAO) as the main base. The environmental aspect of the EAL is that it is > 60% biodegradable according to OECD 301 [8] and contains a certain proportion of renewable products. The commercial PAO and the EAL contain additives with known amounts of sulphur and phosphorus, although full details of the compounds are not known to the authors. The reference oil is PAO-based and contains no additives. It was used merely for identifying the lubrication regime in the ball-on-disc. The pressure viscosity values are unknown to the authors. Thus, the pressure viscosity values are taken from Höglund [9] who presents measured values for various base oils. The reference and commercial oils are both PAO-based, and the EAL is assumed to have the same values as a diester-based oil.

2.3 Test Procedure

Wear tests with no running-in were run at constant rolling speed, loading and slide-to-roll ratio (the reason behind no-running originates from the previous twin-disc study). Five surface/lubricant combinations were tested and each test was repeated three times. The circumferential ground surface was only run with the commercial lubricant and serve as a reference for the computational simulations. All test parameters except the lubricant temperature were set close to the parameters used in the previous study that used a twin-disc set-up [7]. The twin-disc set-up did not allow temperature control, so the inlet temperature of the lubricant applied by drop lubrication on the upper disc was equal to the room

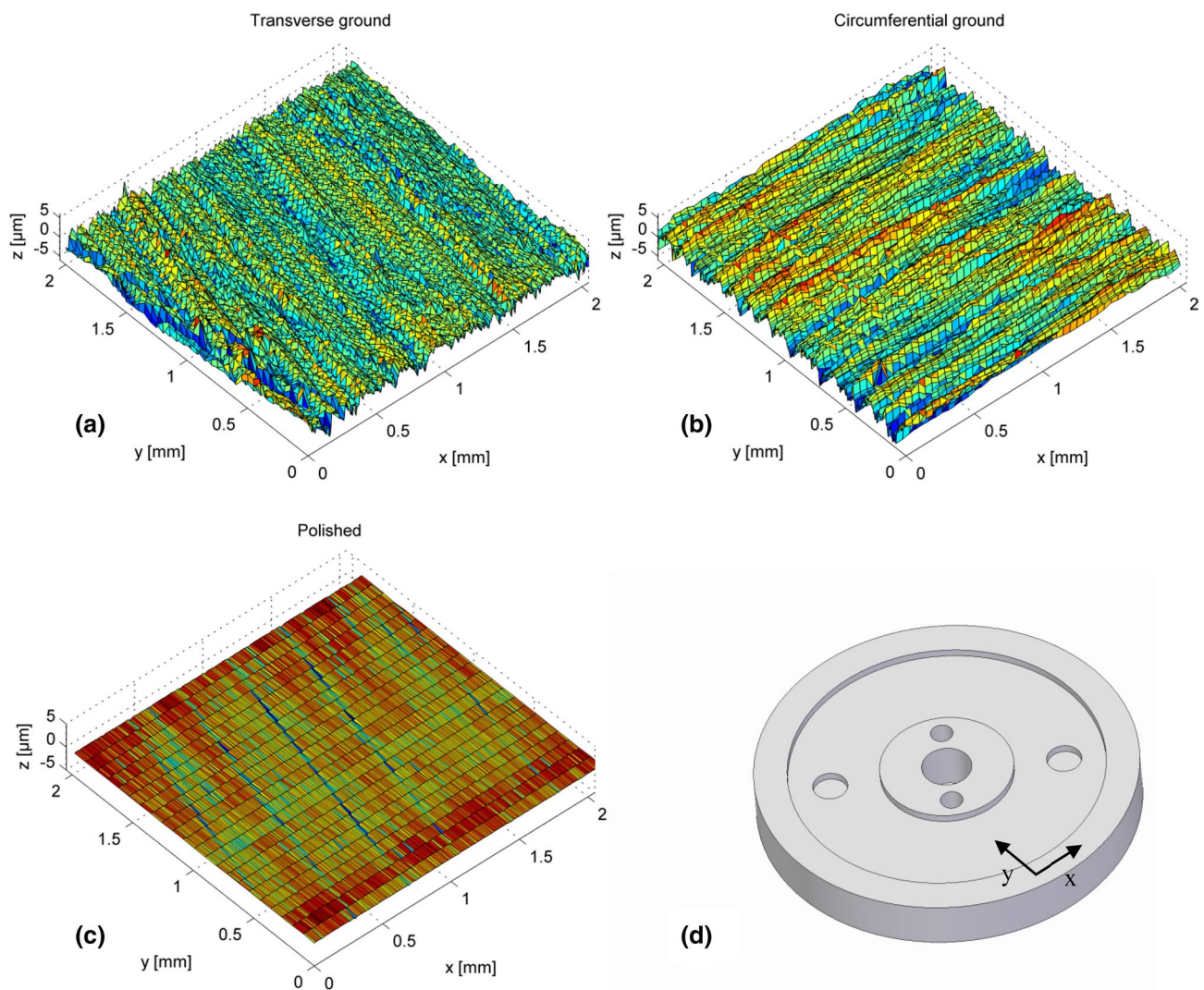


Fig. 3 Surface topography (areas of 2×2 mm) for **a** transverse ground disc, **b** circumferential ground disc, and **c** polished disc. The x -axis corresponds to the sliding direction as indicated on the disc in **d**

Table 1 Characteristic of the reference oil and formulated lubricants

	Reference oil	EAL	Commercial
Dynamic viscosity at 40 °C [mPas], η_{40}	63	69.2	52.3
Dynamic viscosity at 100 °C [mPas], η_{100}	9.1	10.5	9.2
Density [kg/m^3] at 40 °C, ρ_{40}	842	915	820
Density [kg/m^3] at 100 °C, ρ_{100}	805	875	782
Viscosity index [–], VI	137	155	183
Phosphorus content [ppm]	–	1700	300
Sulphur content [ppm]	–	7300	890
Pressure viscosity at 20 °C [GPa^{-1}], α_{20}	15.5*	14.6*	15.5*
Pressure viscosity at 80 °C [GPa^{-1}], α_{80}	10.5*	11.6*	10.5*

*Taken from Höglund [9]

temperature, 20 ± 2 °C. In the ball-on-disc configuration, the temperature was set to 90 °C (which is closer to real gear

operating temperature) and the number of disc cycles was set to 33 000 (the same as for the faster running disc in the

twin-disc set-up). Slip was set to 10%, which represents a value close to the pitch point. The load of 28 N (7.14 kN for the twin-disc set-up) was set to create a maximum Hertzian contact pressure of 2.2 GPa, similar to the FZG load stage 12 in pitting test (2.197 GPa) [10]. All test parameters were kept constant during each run to obtain the most stable and reproducible results. The mean rolling speed was 1.1 m/s. The slip ξ is defined for the ball-on-disc set-up as follows:

$$\xi = 200\% \frac{v_a - v_b}{v_a + v_b} \quad (1)$$

with indexes a and b for disc and barrel speed v , respectively. Before testing, the disc test specimens were cleaned in an ultrasonic bath with heptane followed by methanol and were measured and weighed after 24 h. After testing, the specimens were cleaned using the same procedure.

Partial Stribeck tests were run for all surface and lubricant combinations to determine in which lubricant regime each test combination was run. By the partial Stribeck curve test, we mean that the tests were only run in the boundary and mixed lubrication regimes. The elastohydrodynamic lubrication (EHL) regime was not mapped since the maximum rotational speed of the test rig is reached before surface lift-off. During the partial Stribeck test, the rolling speed is increased while other settings are kept constant.

2.4 Numerical Simulation

The contact was analysed using a numerical model that deals with normally loaded and rolling/sliding contacts using surface topographies as inputs [11]. The surfaces are divided into $i \times j$ rectangular cells (i cells in the x -direction and j cells in the y -direction). The model solves the contact equations by replacing continuous parameters with a unique set of pressures that exactly match the boundary conditions at the centre of the cell. The model considers both normal loading and the effect of slip (rolling/sliding) in the contact.

2.4.1 Normal Loading

A normally loaded contact comprises the interaction of two contact bodies loaded by a normal force. If the asperities are assumed to be small so all pressures act in the normal direction and the materials of the two bodies are assumed to be identical and isotropic, the tangential tractions can be omitted. Knowing the gaps between the cells before deformation, denoted by a vector \mathbf{h} , the unknown pressure \mathbf{p} at all cells can be solved in the matrix form:

$$\mathbf{C}^p \mathbf{p} = \delta_z - \mathbf{h} \quad (2)$$

where \mathbf{C}^p is the influence coefficient matrix. Each component C_{ijp} relates the deformation at element i due to a unit

pressure in cell j . The influence coefficients for a uniform pressure on a rectangular cell were found by Love [12]. The known applied normal force is gained by solving the linear equation system and iteratively varying the applied normal displacement δ_z . As the real contact areas are unknown in advance, it is necessary to start with estimated contact regions. The estimates are obtained as the region one would get if the bodies were penetrating each other without any interactions. Solving Eq. (2) will therefore result in some pressures having negative values, indicating that these elements are outside the contact region. These elements are removed and Eq. (2) is solved again until all pressures become positive. In contacts between rough surfaces it is common that the contact pressure at some asperities exceeds yield stress implying that the resulting deformation is plastic rather than elastic. Marshall et al. [13] proposed an approximation to account for this by including an ideal plastic material model that limits the allowable pressure. Thus Eq. (2) is first solved by removing all negative pressures. Then the pressures within the contact region that exceed the chosen allowable pressure level are known and moved to the right-hand side in Eq. (2). Note that these plastically deformed elements will still contribute to the deformation at the elastic elements. Finally, the iteration is resumed until all the pressures are positive and less than or equal to the allowable pressure.

2.4.2 Slip

In modelling rolling/sliding contact, the contact starts with a stick area and slip occurs when elastic deformation cannot support the relative motion of the two bodies. With increasing tangential displacement, the slip areas increase and stick areas decrease, leading to more tangential force being transmitted. This process continues until gross slip appears. The relationship between micro-slip velocity and the strains in the surface is thoroughly discussed in Johnson [14]. If one observes the contact under the assumption of steady rolling without spin, the integration of an equation found by Johnson expresses the tangential deformation \mathbf{u} as follows:

$$\mathbf{u} = \xi \mathbf{x} - \mathbf{s} + c_0 \quad (3)$$

where ξ is the slip defined as in Eq. (1), \mathbf{x} is the distance to the leading edge, \mathbf{s} is the slip distance, and c_0 is a constant generated from the integration. On the discretised grids, the general equation Eq. (3) is rewritten in matrix form, so that the traction \mathbf{q} is solved by each strip in the rolling direction (thus only j is included):

$$\mathbf{C}^q \mathbf{q} = \xi \mathbf{x} - \mathbf{s} + c_{0j} \quad (4)$$

where \mathbf{C}^q is the influence coefficient matrix that governs the relationship between the tractions and deformations. The

traction on each element $q_{i,j}$ at input pressure $p_{i,j}$ is limited by the limiting coefficient of friction μ_l of that element:

$$q_{i,j} \leq \mu_l p_{i,j} \quad (5)$$

The slip distance s is not really calculated in the solution, since the solution starts with the assumption that there is no slip in the contact area. Once Eq. (4) is solved, the tangential stresses near the trailing edge will violate the limiting friction condition, Eq. (5). These violating elements are then moved to the right-hand side of the equation since the tangential traction is known ($q_{ij} = \mu_l p_{ij}$) and they still affect the remaining elements. Equation (5) will be solved repeatedly until all remaining elements are sticking. Finally, the equation to calculate the coefficient of friction μ_c (the ratio of total tangential force and normal load) is given by:

$$\mu_c = \frac{F_T}{F_N} = \frac{\int q_{i,j} dA_r}{F_N} = \frac{\sum q_{i,j} A_r}{F_N} \quad (6)$$

where F_T and F_N are the traction force and normal force, respectively, and A_r is the area of the contacting cells.

2.5 Computational Set-Up

Simulation results are compared with the tests from current ball-on-disc and the previous twin-disc measurements (Fig. 4). Geometrical contact information for both test configurations using general Hertz contact calculations is presented in Table 2. Given that the contact area is significantly bigger in the twin-disc contact than in the ball-on-disc contact, it is hard to solve rough surfaces with identical resolutions in the twin-disc contact due to the limited number of elements. Therefore, the comparison between the two configurations is made using smooth (nominal) surfaces. Computational comparison using the ball-on-disc contact

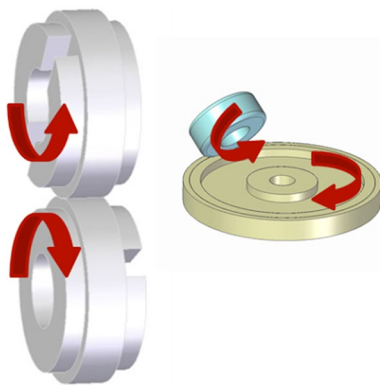


Fig. 4 3D schematic view (not correctly scaled) of the twin-disc (left) and ball-on-disc (right) configurations commonly used to simulate the rolling/sliding gear and wheel–rail contact (arrows indicate the direction of rotation)

Table 2 Contact conditions for the two test set-ups

	Ball-on-disc	Twin-disc
Radius of curvature in x - and y -direction of bodies a and b [mm]	$r_{ax} = inf; r_{ay} = inf; r_{bx} = 9.525; r_{by} = 1$	$r_{ax} = 23.5; r_{ay} = 500; r_{bx} = 23.5; r_{by} = 500;$
(the barrel correspond to body b)		
Elliptical semi-major axis [μm]	162.27	3300
Elliptical semi-minor axis [μm]	37.42	460

with rough surfaces was tested by changing the main surface orientation (i.e. transverse and circumferential), the barrel (body b) is smooth though. The surface topographies are simplified as sinusoidal waviness. The average value of wavelength is 40 μm and amplitude is 1.5 μm ($R_a = 0.95 \mu\text{m}$) based on surface measurements.

The numerical model has a fixed limiting coefficient of friction. The value of the limiting coefficient of friction μ_l can be considered as the maximum value of the coefficient of friction in a stationary lubricated contact. Thus, the contact is not ‘strictly’ dry. This value was set to 0.2 based on the Stribeck tests in the ball-on-disc machine using the transverse ground disc. In order to include the effect of plasticity in the contact, the allowable pressure was set to 4 GPa, which is the maximum nominal (Hertz) pressure used in the bearing industry (the static load capacity for roller bearings is roughly 4 GPa). This value can be used to verify whether the elastic contact model is appropriate, although locally, the real pressures can be much higher than the set limit for plastic deformation.

3 Results

3.1 Stribeck Test Results

Because the two tested lubricants differ in base and additives, a partial Stribeck curve was created for each surface/lubricant combination in order to determine in which lubricant regime each test combination was run (Fig. 5). The speed axis is also plotted in log scale to visualise the boundary regime and to show any transition between lubrication regimes. It can be seen that the EHL regime is not mapped, the maximum rotational speed of the test rig is reached before surface lift-off, the contact experience boundary-to-mixed lubrication. When tested with the reference oil, the ground surface shows significantly different behaviour than when tested with the two formulated lubricants. The lack of additives in the reference oil led to significant amount of metal-to-metal contact. The circumferential ground disc

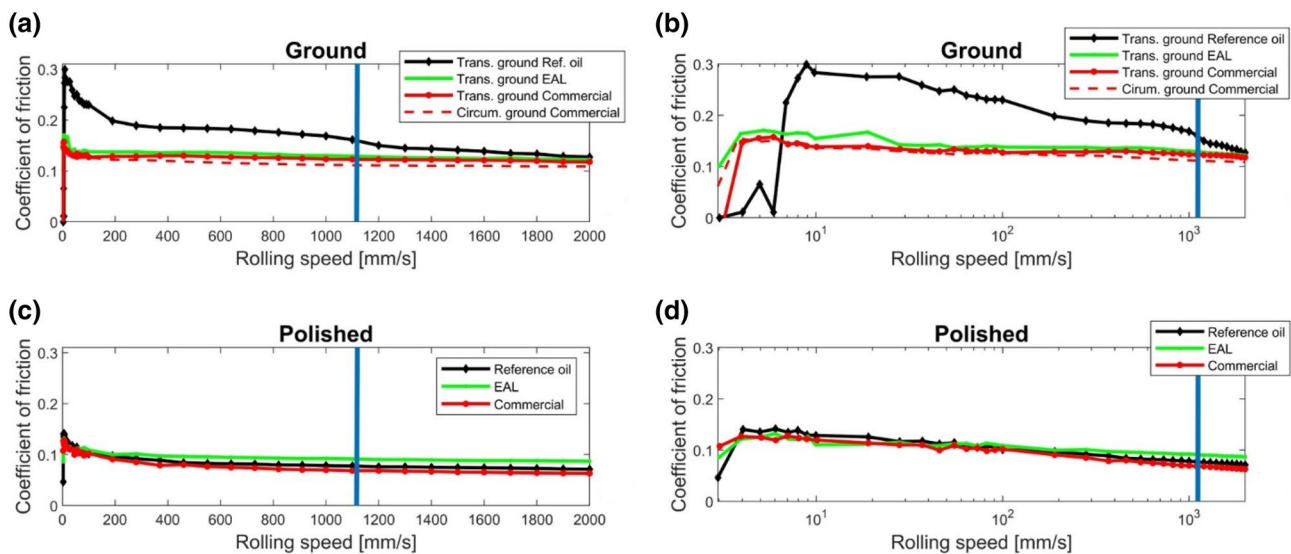


Fig. 5 Partial Stribeck curves. The coefficient of friction versus rolling speed in normal and logarithmical scale axis for ground and polished surfaces. A vertical blue line is drawn in the graphs to indicate the constant rolling speed used for wear tests

Table 3 Film parameter Λ (Appendix A) for different surface/lubricant combinations in ball-on-disc and twin-disc

Λ	Ball-on-disc		Twin-disc	
	Ground	Polished	Ground	Polished
Reference	0.024	0.31	–	–
EAL	0.028	0.36	0.17	2.2
Commercial	0.024	0.31	0.14	1.8

has a slightly lower coefficient of friction than the transverse ground disc. Note that the circumferential ground disc is only tested with the commercial lubricant (Fig. 5a, b). For the polished disc, the reference oil containing no additives shows similar behaviour to the formulated lubricants (Fig. 5c, d). The film parameter is presented in Table 3; see calculations in Appendix A. The EAL, having the highest viscosity, gives a higher film parameter compared to the other oils (Table 1). Table 3 also shows values calculated for the twin-disc set-up.

3.2 Wear Tests at Constant Rolling Speed

Wear tests in the ball-on-disc with no running-in (as the previous study using the twin-disc set-up) were run at constant rolling speed. In Fig. 6, the friction behaviour is presented for each ground surface/lubricant combination, showing one of the three repeated wear tests. The reference oil has the highest starting friction value, but also shows a steep decrease in friction during the first 800 s. This is followed by coarse fluctuations, which stop after approximately half the test time. The other combinations do not

show this behaviour. Instead, after an initial decrease in friction in the first 100–200 cycles, a more or less constant frictional behaviour appears. The circumferential ground surface test with the commercial lubricant shows less fluctuating friction behaviour, and a roughly 3% lower coefficient of friction compared to the transverse ground specimen run with the commercial lubricant at the end of test. Additionally, the noise level (not measured) during these two tests was a major difference. The circumferential ground surface had a significantly lower noise level during testing. The topography in Fig. 6 shows the wear track on the transverse ground surface test with the reference oil; this test track width is almost 200 μm . Figure 7 shows photos of the wear tracks from the tests with the reference oil and the two lubricants on the ground discs. All wear tracks were measured using the stylus instrument and the light optical microscope (mean width of three positions on the disc). However, only the transverse ground discs tested with the reference oil could be accurately measured (the wear track width was observable) using the stylus instrument. The mean width detected in the light optical microscope is shown in brackets. No weight losses on the discs were found.

The polished discs (Fig. 8) are running in a different lubrication regime and show lower friction compared to the ground discs. The friction with the reference oil still has a fluctuating start, and ends with a low coefficient of friction. The topography in Fig. 8 shows the wear track on the polished surface tested with the reference oil. The track width is almost 80 μm , similar to the Hertzian contact width (Table 2). Figure 9 shows photos of the wear tracks.

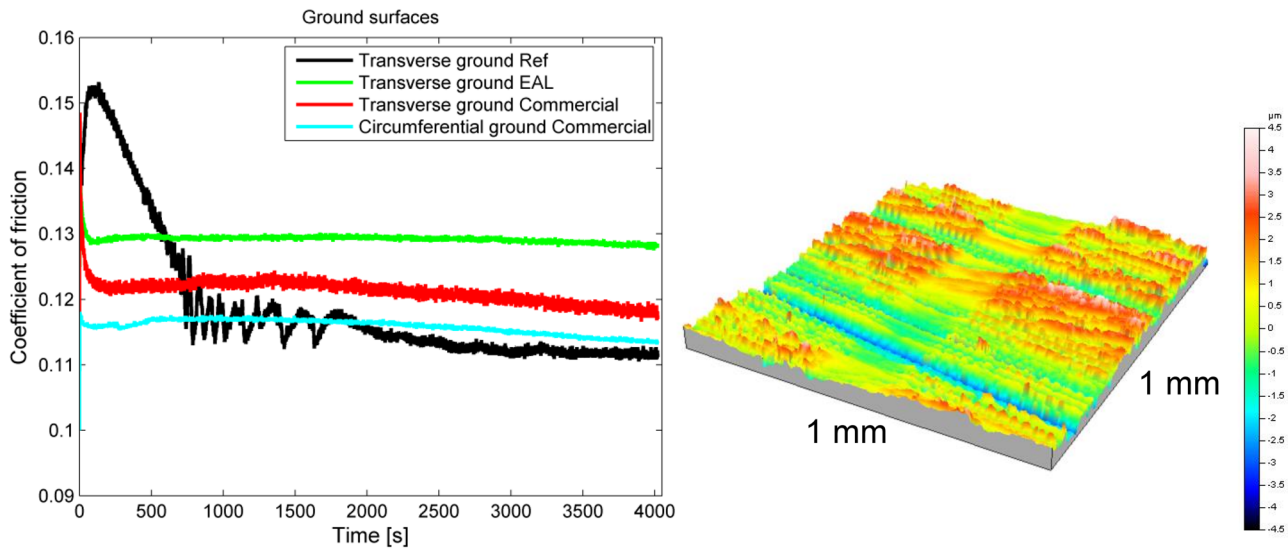


Fig. 6 Coefficient of friction for ground surfaces and a topographical view (10% amplified in height) for the transverse ground surface run with the reference oil (Ref). The topography is shown using centred scaling from -4.5 to 4.5 μm

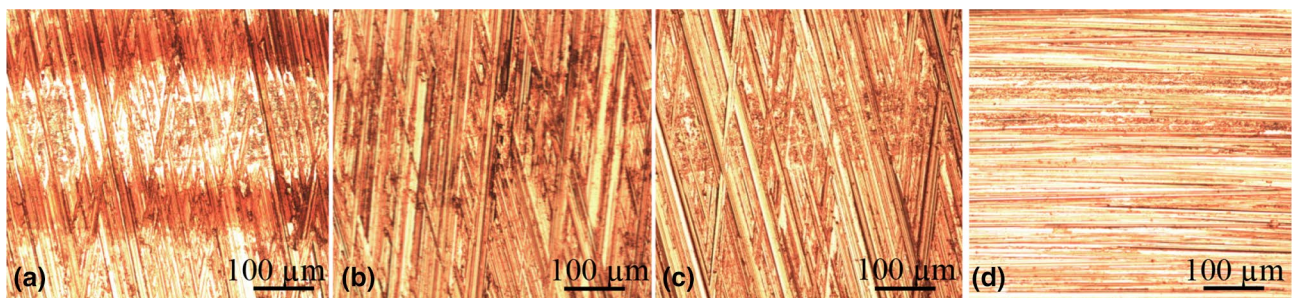


Fig. 7 Light optical microscope photos of wear tracks on the transverse ground surface using **a** reference oil (140 μm), **b** EAL (110 μm), **c** commercial lubricant (100 μm), and **d** commercial lubricant run with circumferential ground surface (100 μm)

3.3 Twin-Disc Results

Twin-disc key results are presented here for a comparison between the present study and the previous study. The twin-disc study made use of the same lubricants and surface finishes as the ball-on-disc study. Table 3 shows calculated film parameters for both set-ups; the polished twin-discs have values around 2. The lubricant efficiently separated the surfaces. To obtain information about the composition of chemically reacted surface layers, the twin-disc specimens were analysed using GD-OES (glow discharge-optical emission spectroscopy). As shown in Fig. 10a, the EAL gives higher friction than the commercial. Surface analysis revealed no notable change in the chemically reacted surface boundary layer of the polished surfaces. Thus, the lubricant properties unknown to the authors are most likely the reason behind this behaviour. For the ground twin-disc surfaces, the EAL additives reacted with the surface to a greater extent than the

commercial lubricant additives. An increase in the boundary layer, using the EAL, which itself needs to be sheared off, can explain the higher friction. However, if active elements are mainly physisorbed to the surface that might be the case for the commercial lubricant; this will not be captured by the GD-OES. Physisorbed layers can, therefore, not be excluded from being the factor lowering the friction of the commercial lubricant. Micropitting was found on all ground surfaces with both lubricants (Fig. 10b). The deepest grinding grooves from the manufacturing process did not disappear.

3.4 Computational Results

The results from the contact simulations at 0.1% slip are summarised in Table 4 and the calculated coefficient of friction versus slip is presented in Fig. 11. With increasing slip, the coefficient of friction of different surfaces first increases (stick-slip) due to the increased slip area and then saturates

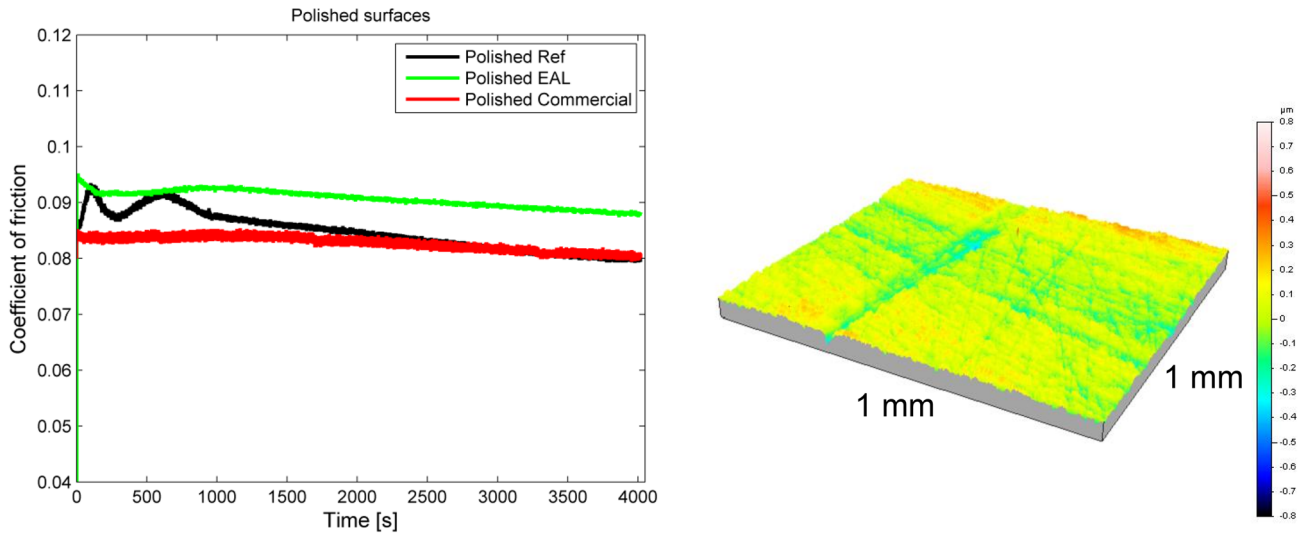


Fig. 8 Coefficient of friction for polished surfaces and a topographical view (10% amplified in height) for the polished surface run with the reference oil (Ref). The topography is shown using centred scaling from -0.8 to $0.8 \mu\text{m}$

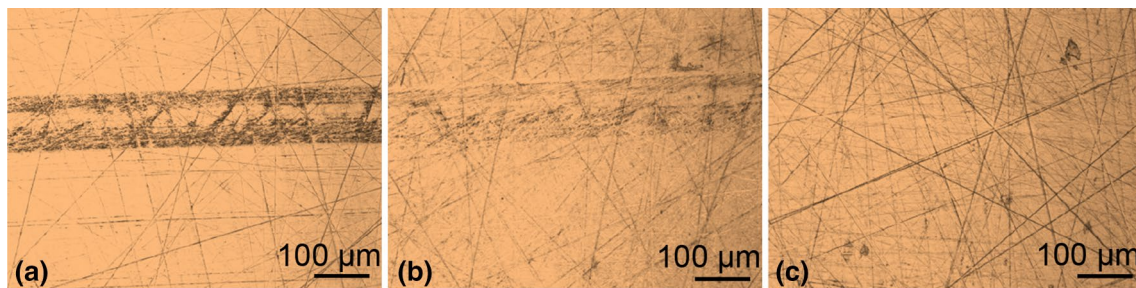


Fig. 9 Light optical microscope photos of wear tracks from the polished surface using **a** reference oil ($95 \mu\text{m}$), **b** EAL ($95 \mu\text{m}$) and **c** commercial lubricant ($-$)

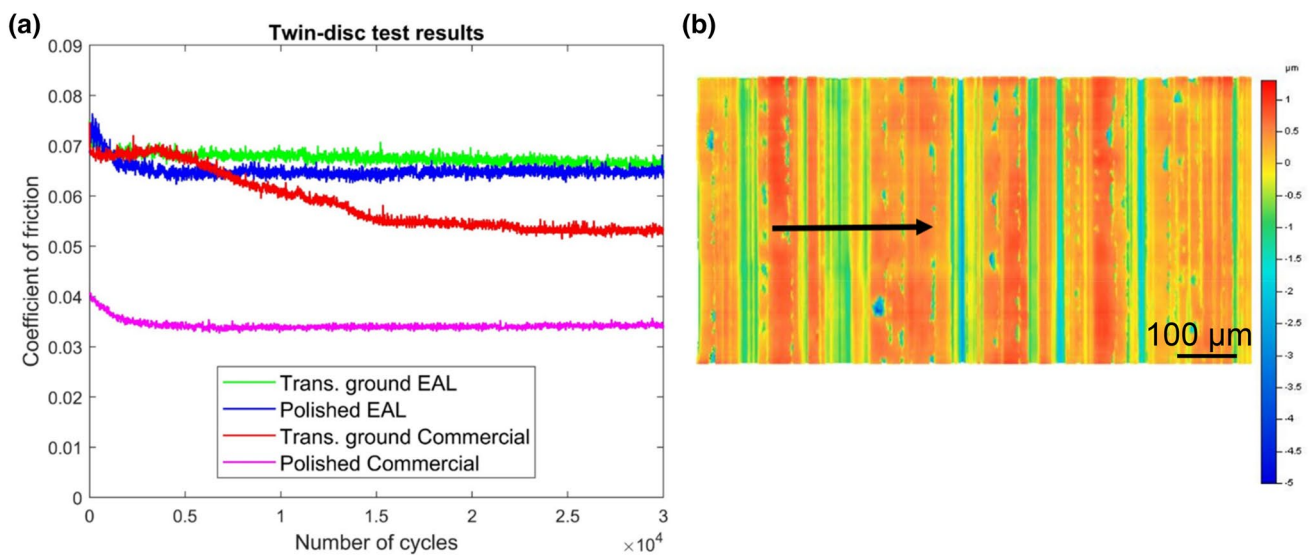


Fig. 10 **a** Coefficient of friction for all surface/lubricant combinations run using the twin-disc machine and **b** a 3D top view image of $0.5 \times 1 \text{ mm}$ area of transverse ground run with commercial. The scale is centred and cover -5 to $1.3 \mu\text{m}$ (arrow indicates the rolling direction)

Table 4 Output from the computer simulation using 0.1% slip. Note that the mean contact pressures are result of the normal loading of 28 (ball-on-disc) and 7140 N (twin-disc), respectively

Configuration	Disc surface	Coefficient of friction μ_c [-]	Real contact area A_r [mm ²]	Mean contact pressure [MPa]	Ratio of cells with $p_0 > 4$ GPa [%]
Ball-on-disc	Polished (smooth)	0.099	0.020	1400	0
Twin-disc	Polished (smooth)	0.056	4.9	1500	0
Ball-on-disc	Transverse ground	0.111	0.0092	3052	62.7
Ball-on-disc	Circumferential ground	0.103	0.0088	3175	64.3

at the set limiting coefficient of friction 0.2 (gross slip). Each curve will eventually reach 0.2 when the friction saturates regardless of test set-up and surface roughness. All contacts saturates before 10% slip is reached. However, their slopes differ at small slip ratios. The ball-on-disc contact saturates before the twin-disc contact. Further, Table 4 shows that the ball-on-disc contact gives a 43% higher calculated friction μ_c than the twin-disc contact for the polished (smooth) surfaces at 0.1% slip. The real contact area, in this smooth case the same as the nominal contact area, is 245 times larger in the twin-disc contact. However, the mean contact pressure is almost identical and none of the contact element cells exceed 4 GPa.

Both rough cases have many parts reaching the set limit for the elastic model to be appropriate, causing much smaller contact area than a polished (smooth) surface does. Even if the transverse texture has higher friction than the circumferential texture at 0.1% slip, after 0.2% slip, the slope decrease more than for the circumferential. The transverse case has more cells in contact that has not yet saturated at 0.1% slip, as can be seen in Table 4. In a numerical simulation, the calculation accuracy can be increased by increasing the number of cells by the sacrifice of computation time. In this study, it was found that having rough surfaces, too coarse cells give

large deviations in terms of plasticity and real contact area compared to fine cells (Appendix B). The results shown in Table 4 are obtained from intermediate cells. For smooth surfaces, including barrel-on-disc contact and twin-disc contact, the coefficient of friction and the real contact area is almost independent of the number of cells.

4 Discussion

In this study, friction and wear tests were conducted in a ball-on-disc, using a barrel instead of a ball to reach contact pressures above 1.25 GPa. This study is partly a follow-up to a previous study that made use of a twin-disc set-up [7]. The same two lubricants and surfaces used in the previous study were used in this ball-on-disc study. The fact that the results obtained with the ball-on-disc did not completely match the results of the previous twin-disc machine led to further investigation. The main dissimilarities between the two set-ups are thus discussed. The contacts resulting from the two set-ups were also compared using a numerical model.

4.1 Influence of Surface Roughness and Lubricant on Friction and Wear Using Ball-on-Disc

The boundary lubrication regime is sometimes defined as the condition in which only the lubricant chemistry (boundary film) determines the friction behaviour, and the fluid film has no effect [15]. The partial Stribeck curves (Fig. 5) suggest that wear tests using the ground discs tested with the two formulated lubricants were mainly run in the boundary lubrication regime, since the reference oil without additives gives a significantly higher coefficient of friction. The Stribeck curves for the polished discs suggest that at testing speed the contact conditions belongs closer to the mixed film lubrication regime, and boundary surface layers do not have same impact as with the ground surface. If this were not the case, the reference oil curve would show a greater difference from the other two friction curves. The film parameter Λ does, however, imply that boundary conditions occur for both surfaces (Table 3).

The wear tests at constant rolling speed show a distinct difference in frictional behaviour between the formulated

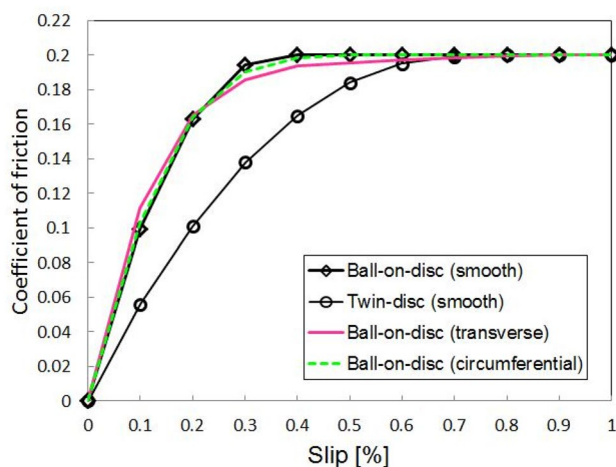


Fig. 11 The coefficient of friction versus slip for the ball-on-disc and twin-disc

lubricants and the reference oil (Figs. 6 and 8). The reference oil shows fluctuating behaviour at the start that can be linked to a change in wear mechanism. The reference oil has not been able to separate the surfaces—the contact has worn through the iron oxide layer. The photo in Fig. 7a also shows fresh ‘shiny’ metal surfaces on the crest of the hills. Moreover, the coefficient of friction is low at end of testing. This could be because at the end the contact is becoming more conformal, since the mean width of the contact is 140 μm , significantly larger than the Hertzian contact width ($\approx 80 \mu\text{m}$). The additives in the lubricants, which the reference oil lacks, controlled the wear process by building up easily sheared boundary layers—thus, the wear tracks are mainly traced by changes in colour (Fig. 7). However, the EAL has a more visible darker layer (Fig. 7b) that suggests that the rate of oxidation has not been slowed down to the same extent as by the commercial lubricant, which most likely has bulk active antioxidants. The EAL also gives a higher friction compared to the commercial lubricant, regardless of surface roughness. The viscosity for the EAL is slightly higher at 100 °C compared to the commercial lubricant (Table 1), but if partial elastohydrodynamic (EHD) lubrication takes place instead of the expected boundary lubrication, lubricant properties unknown to the authors (e.g. pressure viscosity coefficient and limiting shear stress) would best explain the higher coefficient of frictions for the EAL.

For the ground discs, another reason for the difference in friction behaviour with the different lubricants could be the differences in the surface boundary layer, such as layers built up by iron sulphide and metal phosphate [16]. Surface analysis (GD-OES) was performed on the twin-disc surfaces after testing. It showed that the EAL has a thicker reacted surface layer than the commercial lubricant. This thicker layer formed by the EAL did not reduce friction, as this study also suggests, as the boundary layer itself needs to be sheared off. The commercial lubricant may also contain more active elements which are mainly physisorbing to the surface; this will not be picked up by the GD-OES analysis that only captures chemically reacted layers. In other words, the colour shift layers visible in Fig. 7 might not be detected in GD-OES. Physisorbed layers can therefore not be excluded as the factor lowering the friction of the commercial lubricant. The wear on the discs and barrels was hard to quantify as only sporadic local asperity peaks had been removed on the ground discs tested with the formulated lubricants. On the polished discs, the wear track was not measurable using stylus measurements. Moreover, the mass loss of the barrels and discs could not be weighed with sufficient accuracy. An increased number of cycles would probably facilitate the study of the effect of lubricant/surface on wear.

4.2 Surface Roughness Orientation Influence on Friction

Experimentally changing the surface texture orientation to circumferential ground resulted in a lower mean coefficient of friction than when it was transverse ground (Fig. 6). No measurable differences in wear were found, as the mean wear track (distinguished only by colour shifts) was similar for the transverse and circumferential ground disc run with the same lubricant (Fig. 7). The calculated coefficient of friction for the circumferential is also slightly lower at 0.1% slip ratio compared to the transverse (Table 4). Although, after 0.1% slip the friction increases faster (or saturates) compared to the transverse surface (Fig. 11). This can be explained that the real contact area is higher for the transverse case and overweight the influence of mean contact pressure before the friction saturates. The amount of plastic deformation affects the calculation, though. As long as these high pressures ($> 4 \text{ GPa}$) are restricted to a small part of the contact area, their influence on the overall contact is small. However, the high value for plastic deformation suggests that the real contact area is underestimated for both surface textures. Nevertheless, merely adding plastic deformation to the contact model would not greatly affect the results as the lubricant effect would most likely exceed this effect. Figure 13 illustrates the difference in number of wavelengths in contact for the simulated rough ball-on-disc contacts. The limited number of wavelengths in contact for the circumferential ground disc compared to the transverse ground case is noticeable, and thus, the real contact area, regardless of the number of cells in contact (Appendix B), is always higher for the transverse texture.

The calculated friction for the rough surfaces is almost identical to the smooth case (Table 4), which is far different from the experimental testing (ground versus polished, see Figs. 6 and 8). This can be explained by the fact that the computation does not represent a ‘true’ lubricated case. Besides, experimental settings providing mixed to full film lubrication might show more distinct differences depending on surface direction. Johnson and Spence [1] tested transverse and circumferential ground surfaces in a twin-disc rig. Their friction results obtained with the circumferential ground discs were appreciably higher under all conditions (23% on average) than for transversely ground discs. Their explanation is that circumferential roughness permits the oil to pass through the contact in the grooves, leaving the crests of the asperities starved of lubricant. Furthermore, in sliding/rolling conditions, transverse asperities serve to generate micro-EHD lubrication. In this study, the twin-disc contact was only simulated using smooth surfaces. A rough correctly scaled twin-disc contact, using the same sinusoidal wavelength, would exceed the maximum number of pressure cells that a conventional computer can handle.

4.3 Ball-on-Disc Versus Twin-Disc Testing

The mean friction for all surface/lubricant combinations (three repetitions) for the ball-on-disc tests and previous results for twin-disc tests (two repetitions) run under similar conditions is presented in Fig. 12 together with the output from the computer simulation using smooth surfaces. It can be seen that the friction has increased by roughly a factor two for all tests, except for the polished surfaces run with the EAL. The ratios between the mean friction results are similar for all tests, indicating that the ball-on-disc tests properly simulate the same friction trends as in the twin-disc. The calculated coefficients of friction at small slip ratios for smooth specimens show agreement with the experimental ball-on-disc and twin-disc results. Rebbechi [17] measured friction in gears instantaneously and showed coefficient of frictions between 0.04 and 0.06. Johnson and Spence conclude that tooth friction loss can be predicted from twin-disc tests provided that the surface finish of the discs is representative for the gears [1]. In this study, using a ball-on-disc run at the same contact pressure, the friction increased by roughly a factor two compared to the twin-disc test although the surface finish of the ground discs is close to those found in gears. The wear track was hard to quantify on the ball-on-disc specimens; wear volume could not be calculated nor was any mass loss demonstrated. In contrast, the ground twin-disc specimens suffered from micropitting. Thus, these two test set-ups simulate different wear mechanisms. A general discussion is needed comparing the experimental ball-on-disc and twin-disc configurations.

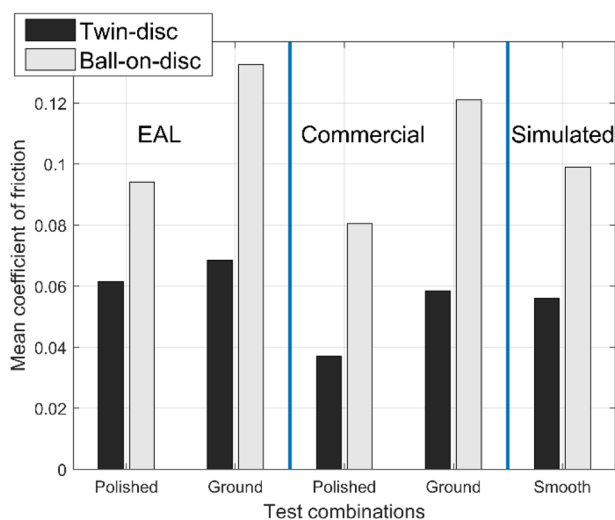


Fig. 12 Mean friction results for twin-disc (at 10% slip) and ball-on-disc tests and simulation (at 0.1% slip)

4.3.1 Temperature

The first striking difference is that the oil bath (or inlet) temperature was 90 °C in the ball-on-disc test compared to room temperature in the twin-disc test inlet. However, two reference tests were performed at 20 °C in the ball-on-disc set-up (not presented) using the transverse ground disc with commercial lubricant. The coefficient of friction increased by approximately 2–5% compared to the tests at 90 °C. Oil bath temperature is therefore not considered to be the main contributing factor for the differences in friction in this study for this number of test cycles. No significant difference in the reference test wear track width was noticed compared to Fig. 7b–d.

4.3.2 Material

In the twin-disc configuration, the two surfaces' material and surface roughness are identical. In the ball-on-disc, the barrel is made of bearing steel with a surface roughness similar to the polished surfaces ($R_a \approx 0.05 \mu\text{m}$). This means that the composite surface roughness $(Rq_a^2 + Rq_b^2)^{1/2}$ is lower for the ball-on-disc configuration (see Appendix A) with the ground surfaces. The hardness of the material is similar for barrel and disc, and generally, barrel bearing steel and gear steel are comparable in chemical composition. Nevertheless, the differences in chemical composition of the steels are not considered to play a significant part in either friction or wear behaviour.

4.3.3 Lubrication

The real gear contact lubricant situation is closer to the twin-disc set-up. The effect of submersion in the lubricant for the ball-on-disc compared to drop lubrication in the twin-disc rig might influence friction. However, this is not noticeable in this study. As shown in the partial Stribeck curves (Fig. 5), the ball-on-disc contact experienced boundary-to-mixed lubrication regime. The EHL regime was not mapped since the maximum rotational speed of the rig is reached before this occurs. The parameters in Table 3 show that running a polished disc in the ball-on-disc is closer to running ground disc surfaces in a twin-disc. One explanation may be that the ratio between the surface peaks and the contact size is more comparable. However, local frictional heating might be a better explanation.

While the nominal contact pressures are more or less the same in the two set-ups, the normal loads are of a completely different magnitude, 28 N (ball-on-disc) and 7140 N (twin-disc), respectively. This difference will give rise to a significant difference in friction heat that is generated in the contacts, which in turn could have a significant influence on the friction behaviour. This heat might have led to lower

viscosities and, consequently, lower friction in the twin-disc contact. Research related to surface treatments for reducing friction shows that thermal phenomenon and chemical/surface interaction play a critical part in lowering the frictional losses [17, 18].

4.3.4 Contact Size and Surface Lay Direction

The contact area is significantly larger (Table 2) in the twin-disc machine; the lubricant has less chance to squeeze out of the twin-disc contact; the lubricant is retained in the area throughout the whole contact. Further, the twin-disc contact has its semi-major contact width parallel to the sliding direction; in the ball-on-disc set-up, the opposite applies. This is schematically illustrated in Fig. 13, which also illustrates the number of wavelengths in contact when the surface direction is opposite to the direction of rolling compared to being in the direction of rolling.

4.3.5 Calculated Coefficient of Friction Versus Experimental

The calculated coefficient of friction of the ball-on-disc configuration increases much faster than that of the twin-disc configuration (Fig. 11). This is most likely linked to the difference in contact geometry, since surface roughness is not included for comparing the set-ups in the simulation (i.e. the surfaces are smooth). The curves of the two test configurations differ only in the small slip area. The reason is the chosen limiting coefficient of friction value and that the stick–slip state may last for a very wide slip range in a real lubricated contact. Besides, selecting another limiting coefficient of friction would not change the small slip area resolution. Note that the calculated coefficient of friction is not intended to directly compared to the experiments in terms of the friction values since the computation does not represent a true lubricated case. According to Zhu [11], under measured oil-lubricated conditions, the friction curve continues to increase from 0 to 100% slip, indicating a wide range of stick–slip state (i.e. it is not fully saturated at 100% slip). Polach [19] shows that the form and the initial slope of the coefficient of friction versus slip curve for wet, dry, or polluted conditions are different. Furthermore, Björling et al. [17] incorporate thermal EHL effects in a numerical

model, validated by experiments, which show a reduction in friction with increased slip ratio.

5 Conclusions

Experimental measurements and computer simulations showed that ball-on-disc and twin-disc set-ups reflect the same friction trends. Thus, both a ball-on-disc and a twin-disc set-up can be used to rank lubricants based on properties related to friction.

However, the friction results differed by a factor of roughly two when the tribometers were set-up to run at the same contact pressure. These results are in agreement with the simulation results at small slip ratios, which showed that the increase is primarily driven by a difference in contact geometry. Further studies are needed to explore the thermal effects on friction.

Compared to twin-disc, wear was hard to detect on the ball-on-disc specimens although they were run in the boundary-to-mixed lubrication regime. Thus, the surface roughness and lubricant impact on wear could not be analysed.

Acknowledgements Open access funding provided by Royal Institute of Technology. We would like to thank Statoil Lubricants for providing some of the test lubricants, Sören Sjöberg for help regarding the disc specimens, and Johan Andersson and colleagues at RISE for help and for letting us use their ball-on-disc and FFI FriText (Grant No 2017-05540) for the opportunity to carry out this work.

Open Access This article is licensed under a Creative Commons Attribution 4.0 International License, which permits use, sharing, adaptation, distribution and reproduction in any medium or format, as long as you give appropriate credit to the original author(s) and the source, provide a link to the Creative Commons licence, and indicate if changes were made. The images or other third party material in this article are included in the article's Creative Commons licence, unless indicated otherwise in a credit line to the material. If material is not included in the article's Creative Commons licence and your intended use is not permitted by statutory regulation or exceeds the permitted use, you will need to obtain permission directly from the copyright holder. To view a copy of this licence, visit <http://creativecommons.org/licenses/by/4.0/>.

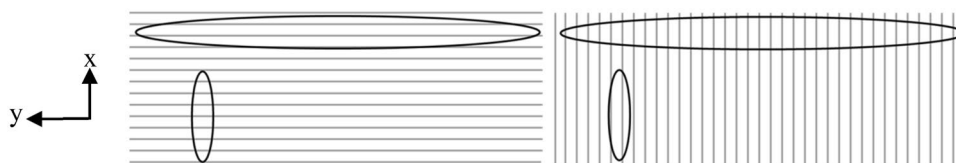


Fig. 13 The transverse case (grey lines, left) and circumferential case (grey line, right) for the two test set-ups. Large ellipse indicates the contact areas of twin-disc while the small ellipse is for ball-on-disc.

(The scaling is not at all representative of the real contact.) The x -axis corresponds to the sliding direction

Appendix A

The minimum film thickness formula given below for EHD lubricated elliptical conjunctions, assuming that the solid surface materials are hard, and that fully flooded lubrication conditions exist, is given by Hamrock [20] as:

$$H = h/R = 3.63U^{0.68}G^{0.49}W^{-0.073}(1 - e^{-0.68k}) \tag{7}$$

The film parameter for the elliptical conjunction is the EHD film thickness for an ideal smoothness of the surfaces divided by the composite surface roughness:

$$\Lambda = h / (Rq_a^2 + Rq_b^2)^{1/2} \tag{8}$$

The input and output data for both test set-ups are presented Appendix in Tables 5 and 6. Note that pure rolling is assumed in the calculations. The dynamic viscosity was measured at 40 °C and 100 °C for each lubricant. However, the pressure viscosity values at 20 °C and 80 °C, respectively, was taken from Höglund [9], since this was not known to the authors. The reference and commercial oils are both PAO-based, and the EAL is assumed to have the same values as the diester-based oil.

Nomenclature for Appendix A

- E* Effective Young’s modulus, $E = 2[(1-\nu_a2)/Ea + (1-\nu_b2)/Eb]-1$ (Pa)
- $E_{a,b}$ Young’s modulus (Pa)
- G* Dimensionless materials parameter ($G = E\alpha$)
- h* Minimum film thickness (m)
- H* Dimensionless film thickness ($H = h/R$)
- k* Ellipticity parameter
- R* Effective radius, $R-1 = [rax-1 + rbx-1]-1 + [ray-1 + rby-1]-1$ (m)
- Rq* RMS roughness parameter (µm)
- U* Dimensionless speed parameter ($U = u\eta_0/ER$)
- u* Mean surface velocity (m/s)

Table 6 Output using EAL values as input. The polished surface in the twin-disc contact made use of a rectangular conjunction

		Ball-on-disc		Twin-disc	
		Ground	Polished	Ground	Polished
<i>E</i>	[GPa]	226			
<i>G</i>		2627	3306	3306	
<i>H</i>		33.6 10 ⁻⁶	22.9 10 ⁻⁶	15.5 10 ⁻⁶	
<i>h</i>	[µm]	0.03	0.26	0.18	
<i>k</i>	[m/s]	4.33	7	7	
<i>U</i>		5.7 10 ⁻¹¹	2.8 10 ⁻¹¹	2.8 10 ⁻¹¹	
<i>W</i>		1.5 10 ⁻⁴	2.18 10 ⁻⁴	2.68 10 ⁻⁴	
Λ		0.028	0.36	0.17	2.2
$(Rqa2 + Rqb2)/2$	[µm]	1.10	0.09	1.56	1.10

- v* Poisson’s ratio
- W* Dimensionless load parameter ($W = wz/ER2$)
- wz* Normal load component (N)
- α* Pressure viscosity coefficient, (Pa⁻¹)
- Λ Specific film thickness
- η_0 Dynamic viscosity (Pas)
- $\omega_{a,b}$ Angular velocity (rad/s)

Index

- a, b* Body *a, b*
- 0 Reference value at atmospheric pressure
- x* Direction of motion
- y* Direction perpendicular to motion
- z* Normal direction

Table 5 Input data, commercial lubricant values in brackets

		Ball-on-disc		Twin-disc	
		Ground	Polished	Ground	Polished
$E_{a,b}$	[GPa]	207			
r_a	[m]	0.021132		0.0235	
<i>R</i>	[mm]	0.9		11.2	
Rq_a	[µm]	1.1	0.06	1.1	0.06
Rq_b	[µm]	0.06		1.1	0.06
<i>U</i>	[m/s]	1.11		1.04	
<i>A</i>	[m ² /N]	1.16 10 ⁻⁸ (1.05 10 ⁻⁸) @ 80 °C		14.6 10 ⁻⁸ (1.55 10 ⁻⁸) @ 20 °C	
$\nu_{a,b}$	[-]	0.293			
w_z	[N]	28		7140	
η_0	[Pas]	0.0105 (0.0092)@100 °C		0.0692 (0.0523)@40 °C	

Table 7 Comparison of the computer simulation with different number of cells

Disc surface	Number of cells	Cell size [$\mu\text{m} \times \mu\text{m}$]	Ratio of cells with $p_{o>4 \text{ GPa}}$ [%]	A_r [mm^2]	Slip [%]	Calculated CoF μ_c [-]
Transverse	1296 (coarse)	20×5	0	0.0136	0.1	0.098
					0.4	0.199
	5041 (intermediate)	10×2.5	62.7	0.0092	0.1	0.111
					0.4	0.194
	19,881 (fine)	5×1.25	56.9	0.0091	0.1	0.111
					0.4	0.194
Circumferential	1369 (coarse)	19.4×5	46	0.0097	0.1	0.104
					0.4	0.2
	3721 (intermediate)	11.7×3	64.3	0.0088	0.1	0.103
					0.4	0.198
	14,641 (fine)	5.8×1.5	73.2	0.0083	0.1	0.099
					0.4	0.197

Appendix B

In a numerical simulation, the calculation accuracy can be increased by increasing the number of cells by the sacrifice of computation time. Table 7 shows how coarse cells give large deviations in terms of plasticity and real contact area A_r compared to fine cells; the coarse cells cannot capture the surface texture. The results based on intermediate cells are acceptable since the real contact area A_r almost reached a steady state with an increased number of cells. When using rectangular shaped cells, there is a small difference in cell size between the transverse and circumferential cases at course, intermediate and fine cells, respectively. However, the number of cells multiplied with cell size is identical for each run simulation.

References

- Johnson, K.L., Spence, D.I.: Determination of gear tooth friction by disc machine. *Tribol. Int.* **24**(5), 269–275 (1991)
- Kleemola, J., Lehtovaara, A.: Experimental simulation of gear contact along the line of action. *Tribol. Int.* **42**, 1453–1459 (2009)
- Björling, M., Miettinen, J., Marklund, P., Lehtovaara, A., Larsson, R.: The correlation between gear contact friction and ball on disc friction measurements. *Tribol. Int.* **83**, 114–119 (2015)
- Vengudusamy, B., Grafl, A., Novotny-Farkas, F., Schöfmann, W.: Comparison of frictional properties of gear oils in boundary and mixed lubricated rolling–sliding and pure sliding contacts. *Tribol. Int.* **62**, 100–109 (2013)
- Björling, M., Larsson, R., Marklund, P., Kassfeldt, E.: Elastohydrodynamic lubrication friction mapping: the influence of lubricant, roughness, speed, and slide-to-roll ratio. *Proc. Inst. Mech. Eng. Part J* **225**(7), 671–681 (2011)
- Höhn, B.-R., Michaelis, K., Kreil, O.: Influence of surface roughness on pressure distribution and film thickness in EHL-contacts. *Tribol. Int.* **39**, 1719–1725 (2006)
- Bergseth, E., Olofsson, U., Lewis, R., Lewis, S.: Effect of gear surface and lubricant interaction on mild wear. *Tribol. Lett.* **48**, 183–200 (2012)
- Guideline for testing of chemicals, information taken from Organisation for Economic Co-operation and Development (OECD) homepage: www.oecd.org (2019). Accessed 27 September 2019.
- Höglund, E.: Influence of lubricant properties on elastohydrodynamic lubrication. *Wear* **232**, 176–184 (1999)
- Höhn, B.-R., Michaelis, K., Otto, H.-P.: Flank load carrying capacity and power loss reduction by minimized lubrication. *Am. Gear Manuf. Association Fall Tech. Meet.* **2010**, 138–152 (2010)
- Zhu, Y.: Adhesion in the wheel-rail contact (PhD dissertation). Stockholm. (2013)
- Love, A.E.H.: Stress produced in a semi-infinite solid by pressure on part of the boundary. *Philos. Trans. R. Soc. Lond. A.* **228**, 377–420 (1929)
- Marshall, M.B., Lewis, R., Dwyer-Joyce, R.S., Olofsson, U., Björklund, S.: Experimental characterization of wheel–rail contact patch evolution. *J. Tribol.* **128**(3), 493–504 (2006)
- Johnson, K.L.: Contact mechanics. Cambridge University Press, Cambridge (2001)
- Totten G.E., (ed). *ASM Handbook, Volume 18, friction, lubrication, and wear technology*, ASM International (2017)
- Torbacke, M., Kassman Rudolphi, Å., Kassfeldt, E.: *Lubricants Introduction to Properties and Performance*. Wiley, Chichester (2014)
- Bobzin, K., Brögelmann, T., Kalscheuer, C., Thiex, M., Ebner, M., Lohner, T., Stahl, K.: A contribution to the thermal effects of DLC coatings on fluid friction in EHL contacts. *Lubr. Sci.* **30**(6), 285–299 (2018)
- Björling, M., Habchi, W., Bair, S., Larsson, R., Marklund, P.: Friction reduction in elastohydrodynamic contacts by thin-layer thermal insulation. *Tribol. Lett.* **53**(2), 477–486 (2014)
- Polach, O.: Creep forces in simulations of traction vehicles running on adhesion limit. *Wear* **258**, 992–1000 (2005)
- Hamrock, B.J.: *Fundamentals of Fluid Film Lubrication*. McGraw-Hill, New York (1994)

Publisher's Note Springer Nature remains neutral with regard to jurisdictional claims in published maps and institutional affiliations.